Inorganic Chemistry

Article

pubs.acs.org/IC

Self-Assembly Synthesis, Structural Features, and Photophysical Properties of Dilanthanide Complexes Derived from a Novel Amide Type Ligand: Energy Transfer from Tb(III) to Eu(III) in a Heterodinuclear Derivative

Cunji Gao,[†] Alexander M. Kirillov,[‡] Wei Dou,[†] Xiaoliang Tang,[†] Liangliang Liu,[†] Xuhuan Yan,[†] Yujie Xie,[†] Peixian Zang,[†] Weisheng Liu,[†] and Yu Tang*[,†]

[†]Key Laboratory of Nonferrous Metal Chemistry and Resources Utilization of Gansu Province, State Key Laboratory of Applied Organic Chemistry, College of Chemistry and Chemical Engineering, Lanzhou University, Lanzhou 730000, P. R. China

[‡]Centro de Quimica Estrutural, Complexo I, Instituto Superior Tecnico, The University of Lisbon, Av. Rovisco Pais, 1049-001 Lisbon, Portugal

Supporting Information

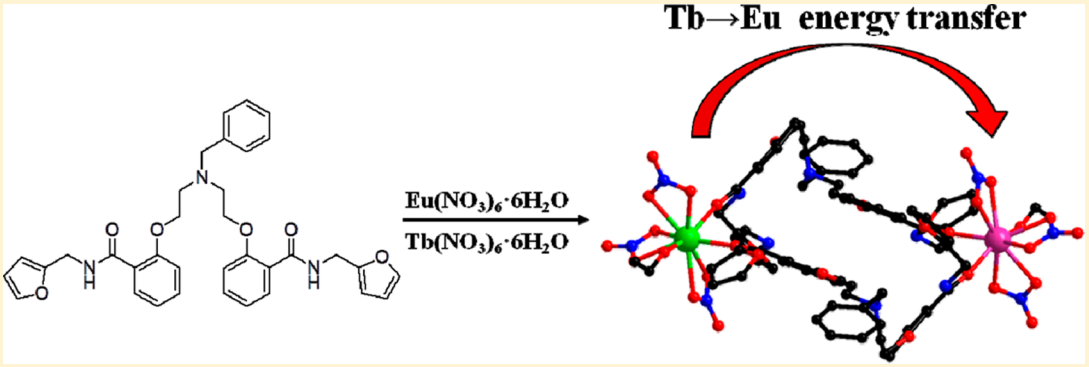

ABSTRACT: A novel amide type ligand benzyl-*N*,*N*-bis[(2′-furfurylaminoformyl)phenoxyl)ethyl]-amine (**L**) has been designed and applied for the self-assembly generation of homodinuclear lanthanide coordination compounds $[Ln_2(\mu_2\text{-}L)_2(NO_3)_6(EtOH)_2]$ [Ln = Eu (**1**), Tb (**2**), and Gd (**3**)] and a heterodinuclear derivative $[EuTb(\mu_2\text{-}L)_2(NO_3)_6(EtOH)_2]$ (**4**). All the complexes have been characterized by the X-ray single-crystal diffraction analyses. They are isostructural, crystallize in a monoclinic space group $P2_1/c$, and form [2 + 2] rectangular macrocycle structures. Compound **4** is the first example of a [2 + 2] rectangular macrocycle heterodinuclear EuTb complex assembled from an amide type ligand. In **4**, the discrete 0D dimeric $[EuTb(\mu_2\text{-}L)_2(NO_3)_6(EtOH)_2]$ units are extended, via the multiple N−H···O hydrogen bonds, into a 2D supramolecular network that has been topologically classified as a uninodal 4-connected underlying net with the **sql** [Shubnikov tetragonal plane net] topology. The triplet state ($^3\pi\pi^*$) of **L** studied by the Gd(III) complex **3** demonstrated that the ligand beautifully populates Tb(III) emission (Φ = 52%), whereas the corresponding Eu(III) derivative **1** shows weak luminescence efficiency (Φ = 0.7%) because the triplet state of **L** has a poor match with $^5D_1$ energy level of Eu(III). Furthermore, the photoluminescent properties of heterodinuclear complex **4** have been compared with those of the analogous homodinuclear compounds. The quantum yield and lifetime measurements prove that energy transfer from Tb(III) to Eu(III) is being achieved, namely, that the Tb(III) center is also acting to sensitize the Eu(III) and enhancing Eu(III) emission in **4**.

INTRODUCTION

Recently, the design of novel lanthanide coordination compounds with conjugated organic ligands has drawn more and more chemists' interests, due to their attractive photophysical properties (large Stokes shifts, long radiative lifetimes, high luminescence quantum yields, narrow bandwidths) suitable for various applications, namely as optical probes, liquid crystalline materials, or biological labeling reagent.[1] Eu(III) and Tb(III) complexes are of special interest because of the high luminescence quantum efficiencies and the versatility of their coordination environments.[2] Among these studies, dinuclear lanthanide coordination compounds attract considerable research interest due to their potential biological,[3] medical,[4] chemical, and technological importance.[5] Energy transfer between two lanthanide ions in heterodinuclear complexes or mixed lanthanide systems has long been known in solution[6] and in the solid state.[7] The use of a second lanthanide ion as an energy transfer acceptor can make the resonance energy transfer measurement more sensitive because

Received: September 16, 2013
Published: January 8, 2014

   dx.doi.org/10.1021/ic402338q | *Inorg. Chem.* 2014, 53, 935−942

the emissions from a donor and an acceptor are readily resolvable as sharply spiked peaks. When the Eu(III) ion is used as an energy receptor from Tb(III), it is common to observe that the luminescence from Eu(III) is strongly sensitized to the detriment of Tb(III) emission.[8] Recent studies have reported the importance of energy transfer modulation between the Tb(III) and Eu(III) ions aiming to obtain solid light-emitting materials and probes based on luminescent switching.[9] Reddy and co-workers have recently reported that the efficient energy transfer (η = 86%) occurs from Tb(III) to Eu(III) in a coordination polymer.[10]

Inspired by the aforementioned progress, we were prompted to design a new ligand with two very flexible amide type arms, namely, benzyl-*N*,*N*-bis[(2′-furfurylaminoformyl)phenoxyl)-ethyl]-amine (**L**) (Scheme 1), and utilized it to construct a

Scheme 1. Chemical Structure of the Ligand L

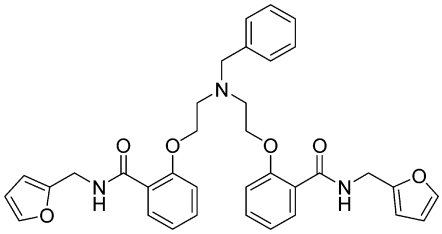

series of new lanthanide coordination compounds $[Ln_2(\mu_2\text{-}L)_2(NO_3)_6(EtOH)_2]$ bearing homodinuclear [Ln = Eu (**1**); Tb (**2**); Gd (**3**)] and heterodinuclear Eu(III)/Tb(III) [Ln = Eu and Tb (**4**)] cations. This semirigid ligand can lead to discrete structures, while the NO_3^- anion can act as a bidentate ligand thus satisfying the need for high coordination number of lanthanide centers. All of the obtained dinuclear complexes have been structurally characterized by X-ray single-crystal diffraction, elemental analysis, and IR spectroscopy. The photoluminescent properties of the dilanthanide complexes have been studied, revealing that the energy can transfer from Tb(III) to Eu(III) and assist sensitization of Eu(III). This will allow modulating the luminescence color by tuning the excitation band or distance between two lanthanide ions in order to design a multicolored light emitter.

RESULTS AND DISCUSSION

Synthesis and Characterization. The homo- and heterodinuclear lanthanide nitrate coordination compounds **1**−**4** were obtained by the self-assembly reaction of lanthanide nitrates with **L** in ethyl acetate. They were isolated as highly air stable powders that are soluble in dimethyl formamide, dimethylsulfoxide, methanol, ethanol, and acetone, slightly soluble in acetonitrile, and insoluble in chloroform and diethyl ether. After two weeks of slow diffusion at room temperature of the diethyl ether to the mixed ethanol and acetonitrile solution of **1**−**4**, the crystals suitable for X-ray analysis were obtained. As a result, single-crystal X-ray structure analyses proved that all the complexes are isostructural. The 1:1 molar ratio of Eu(III)/Tb(III) in a heterometallic compound **4** was further proved by the EDX analysis (Eu/Tb = 0.93; Figure S1 and Table S1 in the Supporting Information). Elemental analysis and IR spectral data for the complexes **1**−**4** are listed in Table 1. In the FTIR spectra, the peak at 1640 cm^{-1} which is assigned to the vibration absorption of a carbonyl group of **L** is replaced by a new absorption peak at 1615−1620 cm^{-1} in complexes **1**−**4** (Figure S2 in Supporting Information), suggesting that the oxygen atoms of the carbonyl groups are coordinated to the central lanthanide ions.

Thermal Stability Studies. To study the thermal stabilities of the complexes **1**−**4**, thermogravimetric analyses (TGA) and differential scanning calorimetry (DSC) were performed on the crystalline samples (Figure S3 in Supporting Information). All the compounds easily lose the crystallization ethanol molecules, the complete elimination of which is observed at 203 °C for **1** (calcd, 4.71%; found, 5.06%), 200 °C for **2** (calcd, 4.67%; found, 4.98%), 227 °C for **3** (calcd, 4.68%; found, 5.03%), and 192 °C for **4** (calcd, 4.69%; found 4.53%). After reaching these temperatures, the compounds begin to decompose, resulting in a concomitant elimination of the two **L** moieties and three nitrate groups (e.g., calcd, 79.69%; found, 78.17% for **1**; calcd, 79.41%; found, 77.95% for **4**). The decomposition process is essentially complete at 600 °C for all the samples.

Crystal Structure Descriptions. The single-crystal X-ray analyses of the complexes **1**−**4** confirm that they are all isostructural dinuclear derivatives and bear the nine-coordinate metal centers. Their coordination environments are filled by two O atoms from carbonyl groups of two μ_2-**L** moieties, six O atoms from three bidentate nitrate groups, and one O atom from the terminal coordinated ethanol molecule. The structural analyses unambiguously prove that the complexes **1**−**4** form discrete [2 + 2] rectangular macrocycles with the sizes 7.246 × 7.557 $Å^2$ (**1**), 7.522 × 7.256 $Å^2$ (**2**), 7.226 × 7.546 $Å^2$ (**3**), and 7.264 × 7.546 $Å^2$ (**4**), respectively. Compound **4** represents the first example of a [2 + 2] rectangular macrocycle EuTb heterodinuclear complex assembled from an amide type ligand.

The molecular structure of **1** shows that two μ_2-**L** ligands adopt a face-to-face orientation and are linked together by two Eu(III) ions, generating a discrete zero-dimensional (0D) dinuclear rectangular macrocycle structure (Figure 1). Each discrete unit consists of two independent Eu(III) centers. As shown in Figure S4 (Supporting Information), the μ_2-**L** moieties reveal the intramolecular π−π interactions of the two benzene ring planes which are parallel to each other, with the centroid to centroid distance of 3.749 Å. Besides, two benzene rings from two arms of each ligand interact through the C−H···π interactions referred as a T-shape arrangement. The coordination polyhedron around Eu(III) is a distorted tricapped trigonal prism. The distance between two Eu(III) ions is 13.243 Å. In addition, the discrete dinuclear units are further assembled into a two-dimensional (2D) supramolecular

Table 1. Elemental Analysis and IR Spectral Data of Complexes 1−4

	found (calcd) (%)				
complex	C	H	N	Ln	IR (cm^{-1}) ν (C═O)
1	45.02 (45.45)	3.83 (4.23)	8.42 (8.60)	15.25 (15.55)	1615
2	44.83 (45.13)	3.76 (4.20)	8.44 (8.53)	15.88 (16.14)	1620
3	44.89 (45.21)	3.75 (4.20)	8.24 (8.55)	15.86 (16.00)	1615
4	44.97 (45.29)	3.76 (4.21)	8.25 (8.46)	Eu 7.24 (7.75)	1618

dx.doi.org/10.1021/ic402338q | *Inorg. Chem.* 2014, 53, 935−942

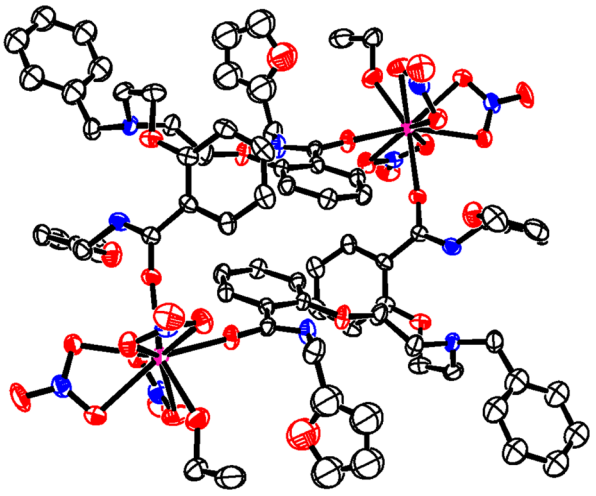

Figure 1. Thermal ellipsoid (30% probability level) plot of complex **1**. All hydrogen atoms were omitted for clarity. Color scheme: gray, C; red, O; blue, N; pink, Eu.

structure through intermolecular hydrogen bonds. Hydrogen bonding parameters in **1** are given in Table S2 (Supporting Information). The crystal structures of **2** and **3** are essentially similar to that of **1** and are thus not discussed.

The structure of the heterodinuclear complex **4** (Figure 2a) resembles those of homodinuclear analogues **1**−**3**. However, in **4** each lanthanide element site is populated by a half Eu(III) and a half Tb(III), so each crystal unit contains one Eu(III) and one Tb(III) atom. Two μ_2-**L** ligands adopt a face-to-face orientation and are coordinated by two metal centers generating a discrete 0D heterodimetallic rectangular macrocycle structure.

In **4**, each dinuclear [EuTb(μ_2-L)$_2$(NO$_3$)$_6$(EtOH)$_2$] block is linked to four adjacent ones via the intermolecular N3−H3A···O11 [3.062 Å] hydrogen bonds (Figure 2b, Table S2 in Supporting Information), thus giving rise to the generation of a H-bonded 2D layer. To better understand the structure of this H-bonded network, we have carried out its topological analysis[11] following the concept of the simplified underlying net.[12] Thus, the molecular units [EuTb(μ_2-L)$_2$(NO$_3$)$_6$(EtOH)$_2$] have been reduced to the respective centroids and considered as the 4-connected nodes. The obtained underlying network (Figure 2c) has been analyzed from the topological viewpoint, revealing a uninodal 4-connected net with the **sql** [Shubnikov tetragonal plane net] topology described by the point symbol of $(4^4{\cdot}6^2)$.[11,13] Although various Eu or Tb containing **sql** nets have been identified,[14] to our knowledge, coordination compound **4** represents the first heterometallic EuTb network of this topological type.[11,15]

Photoluminescent Properties of the Complexes. The excitation and emission spectra of the homodinuclear complexes **1**, **2**, and heterodinuclear analogue **4** were recorded on the crystalline samples at room temperature, and the relevant photophysical data are summarized in Table S3 (Supporting Information). The excitation spectrum of **1** (Figure 3) illustrates that the $^7F_0{\rightarrow}{}^5D_4$, $^7F_0{\rightarrow}{}^5G_{0-4}$, $^7F_0{\rightarrow}{}^5L_6$, $^7F_0{\rightarrow}{}^5D_{2,1}$ and $^7F_1{\rightarrow}{}^5D_1$ excitation bands of Eu(III) ion are more intense than excitation band of **L**,[16] thus proving that the luminescence sensitization through direct excitation of the central Eu(III) ion is much more efficient than **L**. The emission spectrum of **1** was detected at 327 nm which is the maximum excitation wavelength of **L**. Maximum intensities situated at 579, 591, 617, 649, 689, and 701 nm, respectively, were observed for the $^5D_0 \rightarrow {}^7F_J$ (J = 0, 1, 2, 3, and 4) transitions, and

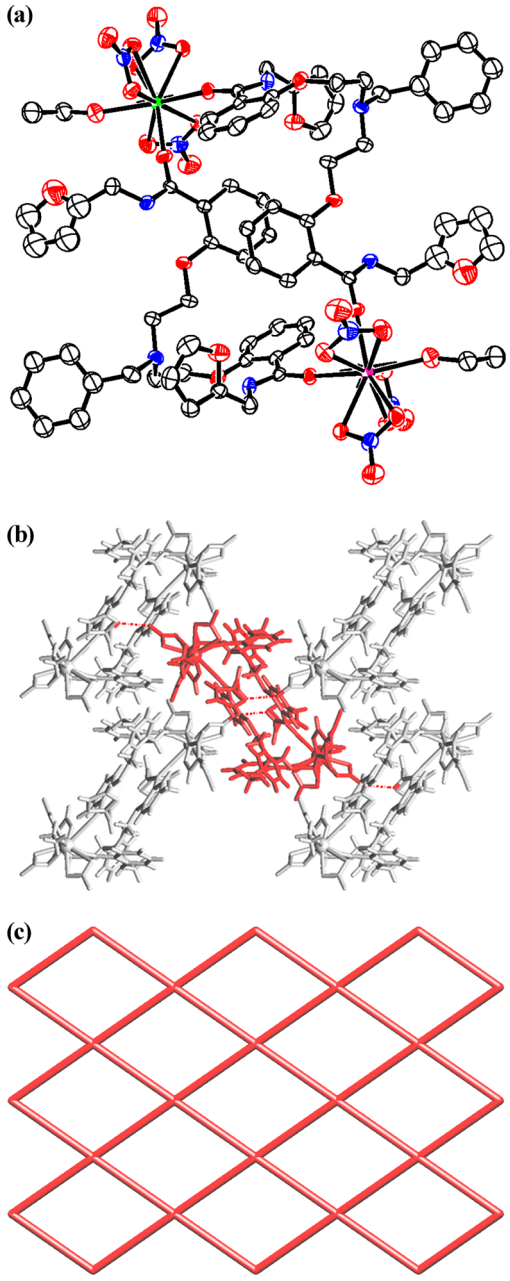

Figure 2. Structural fragments of **4**: (a) thermal ellipsoid (30% probability level) plot of the discrete dinuclear unit. All hydrogen atoms were omitted for clarity. Color scheme: gray, C; red, O; blue, N; pink, Eu; green, Tb. (b) Linkage of the "central" (red) dinuclear unit with four adjacent ones (gray) via the intermolecular N3−H3A···O11 hydrogen bonds (dotted lines), forming a H-bonded 2D layer. (c) Topological representation of the underlying uninodal 4-connected net with the **sql** topology and the point symbol of $(4^4{\cdot}6^2)$; centroids of the [EuTb(μ_2-L)$_2$(NO$_3$)$_6$(EtOH)$_2$] nodes are depicted in red. (b, c) Views along the *a*-axis.

two splitting peaks of the $^5D_0{\rightarrow}{}^7F_4$ transition occur at 689 and 701 nm. The hypersensitive transition $^5D_0 \rightarrow {}^7F_2$ locating at 617 nm is a strong band, leading to a red luminescence emission of **1**.[17] The intensity ratio of $I(^5D_0 \rightarrow {}^7F_2)/I(^5D_0 \rightarrow {}^7F_1)$ about 5.1 indicates that Eu(III) ions in **1** occupy sites with low symmetry and have no inversion center,[1e,18] which is in agreement with the crystal structure analysis.

Figure 4 describes the steady-state excitation and emission spectra of the Tb(III) complex at room temperature. The

dx.doi.org/10.1021/ic402338q | *Inorg. Chem.* 2014, 53, 935−942

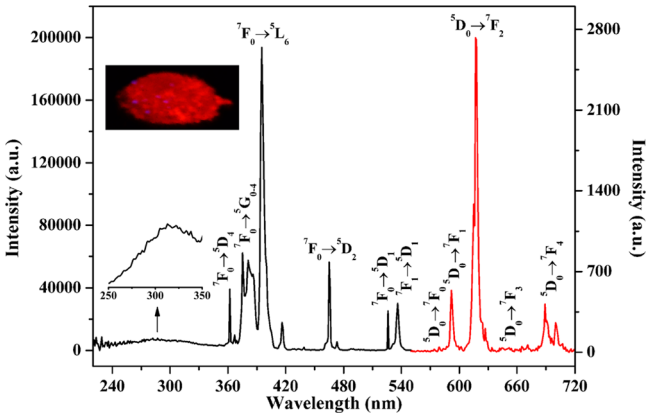

Figure 3. Excitation (λ_{em} = 618 nm) and emission (λ_{ex} = 327 nm) spectra for complex **1** recorded on the crystalline sample at room temperature. Inset image refers to a red emission in **1** under the 365 nm UV lamp.

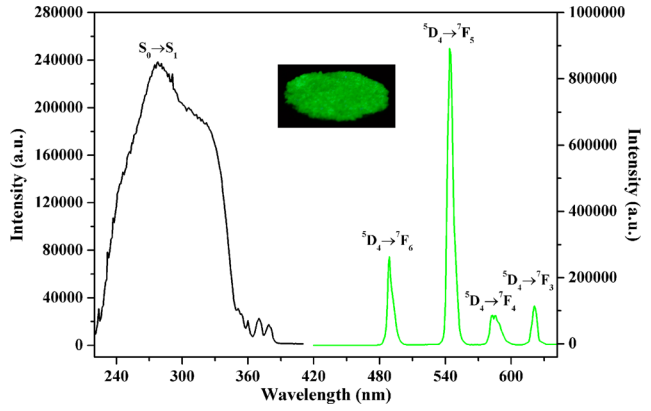

Figure 4. Excitation (λ_{em} = 544 nm) and emission (λ_{ex} = 327 nm) spectra for complex **2** recorded on the crystalline sample at room temperature. Inset image refers to a green emission in **2** under the 365 nm UV lamp.

excitation spectrum is a broad band from 220 to 350 nm, which is associated with the electronic absorption of the ligand. This proves **L** can effective populate the Tb(III) complex. The emission spectrum of **2** shows four characteristic peaks resulting from the $^5D_4 \rightarrow {}^7F_J$ (J = 6, 5, 4, 3) transitions.[19] The most intense one lying at 544 nm agrees with the $^5D_4 \rightarrow {}^7F_5$ transition. Moreover, there is an efficient ligand-to-metal energy-transfer process in this complex proved by the absence of the emission of **L**.

Figure 5 shows the photoluminescent emission spectrum of heterodinuclear compound **4** accompanied by the emission spectrum of **1**, which were recorded in the 450−720 nm range upon excitation at 327 nm at room temperature. Upon ligand excitation, the EuTb derivative **4** displays both the Eu(III) ($^5D_0 \rightarrow {}^7F_J$) and Tb(III) ($^5D_4 \rightarrow {}^7F_J$) transitions. Complex **4** exhibits enhanced luminescence intensity at 617 nm (2.1-fold) corresponding to the $^5D_0 \rightarrow {}^7F_2$ transition of Eu(III) ion compared to that of compound **1**. The presence of Tb(III) enhances the luminescence intensity of the Eu(III) emission. On the other hand, the luminescence intensity at 544 nm of the $^5D_4 \rightarrow {}^7F_5$ transition decreases 41.8-fold in comparison with that of complex **2**, which indicates the relatively high efficiency of Tb(III) → Eu(III) energy-transfer. It is possible that the presence of Eu(III) in the heterodinuclear complex **4** diverts a

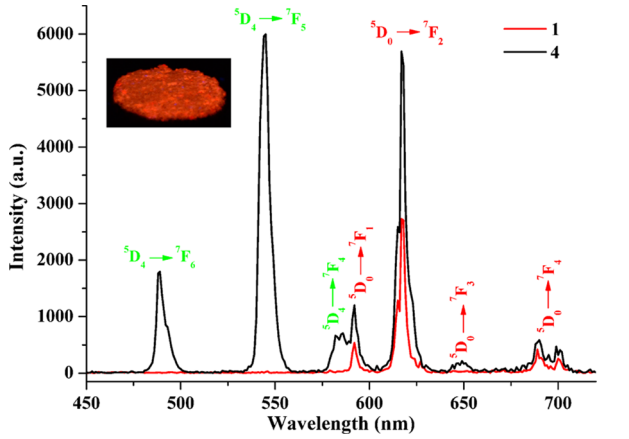

Figure 5. Emission spectra of complexes **1** (red line) and **4** (black line), λ_{exc} = 327 nm recorded on the crystalline sample at room temperature. Inset image refers to a dull-red emission in **4** under the 365 nm UV lamp.

large portion of the energy from the $^5D_4$ level of the Tb(III) ion, thus promoting its fast luminescence quenching. Furthermore, the color in the luminescence image of the heterodinuclear compound **4** shows a dull-red emission under the 365 nm UV lamp (Figure 5).

Energy Transfer from Tb(III) to Eu(III) in Heterodinuclear Compound 4. It is well-known that energy transfer from the triplet state of the ligand to the resonance level of the Ln(III) ion is regarded as an important factor influencing the luminescent properties of lanthanide complexes.[20] To elucidate the energy transfer process in **4**, the singlet energy level of the ligand **L** has been determined by the UV−vis absorption spectrum of the complex **3**, which was measured in methanol solution at room temperature. The wavelength of the absorbance edge of complex **3** is 313 nm (Figure S5 in Supporting Information), indicating that its singlet energy level ($^1\pi\pi^*$) is 31 949 cm^{-1}. Furthermore, we have used the compound $[Gd_2(\mu_2\text{-}L)_2(NO_3)_6(EtOH)_2]$ (**3**) to discuss the triplet energy level ($^3\pi\pi^*$) of the ligand **L**, aiming at assessing its efficiency in the energy-transfer process to the central lanthanide ions. The phosphorescence spectrum of **3** was measured at 77 K in a methanol−ethanol solution (1:1 v/v) (Figure S6 in Supporting Information). As a result, the triplet energy level ($^3\pi\pi^*$) of **L**, corresponding to its lower-wavelength emission edge, is 24 631 cm^{-1} (406 nm). It is interesting to note that the $^3\pi\pi^*$ of this newly designed ligand lies well above the lowest excited resonance level $^5D_1$ of Eu(III) (19 000 cm^{-1}) and $^5D_4$ of Tb(III) (20 500 cm^{-1}). Thus, the absorbed energy of ligand **L** could be transferred to the central Eu(III) and Tb(III) ions. Reinhoudt's empirical rule[21] states that ligand-to-metal energy transfer becomes effective when $\Delta E(^1\pi\pi^* - {}^3\pi\pi^*)$ is at least 5000 cm^{-1}. The energy gap between $^1\pi\pi^*$ and $^3\pi\pi^*$ for the ligand **L** is 7318 cm^{-1}, thus pointing out that this newly designed ligand has a relatively good intersystem crossing efficiency. On the other hand, it is very important that there is a suitable energy gap between the $^3\pi\pi^*$ and the lanthanide ion emissive states since the lanthanide ion emissive states must be efficiently populated for the emission to occur. The empirical rule proposed by Latva[22] states that an optimal ligand-to-metal energy transfer process for a lanthanide ion needs [$\Delta E = E(^3\pi\pi^*) - E(^5D_J)$] of 2500−4000 cm^{-1} for Eu(III) and 2500−4500 cm^{-1} for Tb(III). The calculation of such parameters

dx.doi.org/10.1021/ic402338q | Inorg. Chem. 2014, 53, 935−942

Table 2. Radiative (A_{RAD}) and Nonradiative (A_{NR}) Decay Rates, $^5D_0/^5D_4$ Lifetimes (τ_{obs}), Radiative Lifetimes (τ_{RAD}), Intrinsic Quantum Yields (Φ_{Ln}), Energy Transfer Efficiencies (Φ_{sen}), and Overall Quantum Yields ($\Phi_{overall}$) for Complexes 1 and 2

complex	A_{RAD} (s^{-1})	A_{NR} (s^{-1})	τ_{obs} (μs)	τ_{rad} (μs)	Φ_{Ln} (%)	Φ_{sen} (%)	$\Phi_{overall}$ (%)
1	443	2742	314 ± 3 858 ± 5[b]	2257	14	5	0.7[a]
2			947 ± 2	1116 ± 1	85	62	52[a]

[a]Absolute quantum yield. [b]τ_{obs} at 77 K.

indicates that ΔE is 4131 cm^{-1} for Tb(III), which indicates energy absorbed by **L** can transfer to Tb(III) efficiently.[23] By contrast, ΔE is 7331 cm^{-1} for Eu(III), thus indicating that the ligand **L** cannot populate Eu(III) efficiently.

The overall luminescence quantum yields, Φ, of **1**, **2**, and **4** in the solid state were found to be 0.7%, 52%, and 2.5%, respectively, using an integrating sphere when excited at 327 nm. Lifetime values of two homodinuclear lanthanide coordination compounds **1** and **2**, and heterodinuclear lanthanide derivative **4**, were measured in order to get further insight into the light-conversion processes and to determine the mechanism of the Tb → Eu energy transfer.

The $^5D_0$ (Eu^{3+}) and $^5D_4$ (Tb^{3+}) lifetime values (τ_{obs}) were determined from the luminescence decay profiles for the complexes **1** and **2** at both 298 and 77 K monitored within the more intense lines of the $^5D_0 \rightarrow {}^7F_2$ and $^5D_4 \rightarrow {}^7F_5$ transitions, respectively (Figures S7–S9 in Supporting Information), and the relevant data are listed in Table 2. The shorter $^5D_0$ lifetime (τ_{obs} = 314 ± 3 μs) is detected for complex **1** at 298 K. The lifetime is two component corresponding to two exponential functions ($\langle\tau_{obs}\rangle$ = 858 ± 5 μs) at 77 K indicating the presence of two emissive Eu^{3+} centers.[24] The temperature dependent lifetime reflects the thermally activated deactivation processes.[25] The observed luminescence decay profiles of complex **2** corresponding to single exponential functions at 298 K (τ_{obs} = 947 ± 2 μs) demonstrate the existence of one emissive Tb^{3+} center. The shorter $^5D_0$ lifetimes detected for the Eu^{3+} complex **1** may be caused by the dominant nonradiative decay channels associated with vibronic coupling due to the coordinated solvent molecules. On the other hand, a longer $^5D_4$ lifetime value at 298 K (τ_{obs}= 947 ± 2 μs) has been gained for the Tb^{3+} complex even though there is a solvent molecule in the first coordination sphere since the vibrational deactivators of the excited states of Ln^{3+} ions are present.[25b,26] The $^5D_4$ lifetime values of Tb(III) complex **2** indicate that it is essentially temperature independent because of τ_{RAD} decreasing by ~15%, while temperature goes down from 298 to 77 K. These observations indicate that the Tb(III) complex lacks thermally activated deactivation processes.

The emission of complexes **1** and **2** can be analyzed in terms of eq 1 where $\Phi_{overall}$ and Φ_{Ln} are the ligand-sensitized and intrinsic luminescence quantum yields of Ln(III); Φ_{sen} is the efficiency of the energy transfer from ligand to Ln(III), and τ_{obs}/τ_{RAD} are the observed and the radiative lifetimes of Ln(III).[27]

$$\Phi_{overall} = \Phi_{sen}\Phi_{Ln} \quad (1)$$

Φ_{Ln} can be obtained by the following eq 2:

$$\Phi_{Ln} = \tau_{obs}/\tau_{RAD} \quad (2)$$

For the Eu(III) complex, the radiative lifetime (τ_{RAD}) can be calculated from eq 3,[28] where n is the refractive index (1.5 for solid state metal–organic complexes).[29] $A_{MD,0}$ (14.65 s^{-1}) is the spontaneous emission probability for the $^5D_0 \rightarrow {}^7F_1$ transition in vacuo, and I_{TOT}/I_{MD} shows the ratio of the total integrated intensity of the corrected Eu(III) emission spectrum to the integrated intensity of the magnetic dipole $^5D_0 \rightarrow {}^7F_1$ transition:

$$A_{RAD} = 1/\tau_{RAD} = A_{MD,0} \times n^3 \times (I_{TOT}/I_{MD}) \quad (3)$$

The intrinsic quantum yield for Tb^{3+} (Φ_{Tb}) estimated through eq 4 is 85% on the basis of the hypothesis that the decay process at 77 K in a deuterated solvent is purely radiative.[30,20e]

$$\Phi_{Tb} = \tau_{obs(298K)}/\tau_{obs(77K)} \quad (4)$$

The calculated intrinsic quantum yields and energy transfer efficiencies data for complexes **1** and **2** are listed in Table 2. Poor sensitization efficiency existed in the Eu^{3+} complex mainly because of the larger energy gap between $^3\pi\pi^*$ and the excited $^5D_0$ energy level.

Hence, the luminescence lifetime value of heterodinuclear derivative **4** attained 0.792 ± 0.004 ms ($^5D_0$) and 0.915 ± 0.002 ms ($^5D_4$) from the luminescent decay profiles by both fitting with monoexponential curve (Figure S10 in Supporting Information), indicating the single chemical environment around the emitting lanthanide ions. The lifetime of Eu(III) in **4** almost doubled because of the deceasing concentration of Eu^{3+} ions, and the energy-transfer from Tb^{3+} to Eu^{3+} in this heterodinuclear derivative. The lifetime of the central Tb^{3+} ions in **4** decreases moderately, which may be caused by the following two reasons: (1) The Eu^{3+} reduces the concentration quenching effect between the Tb^{3+} ions, and the decrease of the concentration of Tb^{3+} in complex **4** may give rise to the increased lifetime of Tb^{3+}. (2) The $Tb^{3+} \rightarrow Eu^{3+}$ energy transfer leads to the decreased lifetime of Tb^{3+} ions. The observed change in lifetimes of the Tb(III) and Eu(III) emission in a EuTb heterodinuclear complex, compared to that of pure Tb(III) and Eu(III) emission, further proves that the energy transfer between Tb(III) and Eu(III) indeed exsits. If the main mechanism of the energy transfer process would be dipole–dipole, the through-space energy-transfer effiency can be estimated by the following eq 5:

$$\eta = 1 - (\tau/\tau_0) = 1/[1 + (R/R_0)^6] \quad (5)$$

Here, τ is the Tb($^5D_4$) lifetime in the EuTb heterodinuclear complex, τ_0 is the lifetime in the pure Tb($^5D_4$) complex, R is the Eu···Tb separation, and R_0 is the critical distance for 50% transfer.[31] The energy-transfer efficiency is calculated to be 3% using the above equation when τ = 0.915 ± 0.002 ms and τ_0 = 0.947 ± 0.002 ms. The value for R_0 generally lies between 8 and 10 Å for Eu(III)–Tb(III) pairs.[32] Using a value of 13.2 Å for R and an average value of 9.0 Å for R_0 with the above equation, we obtained a theoretical energy-transfer efficiency of η = 9.1%. Also, this efficiency resembles the one calculated by the experimental lifetime values of complex **4**. Hence, we can conclude that the main energy-transfer path is a dipole–dipole

dx.doi.org/10.1021/ic402338q | Inorg. Chem. 2014, 53, 935–942

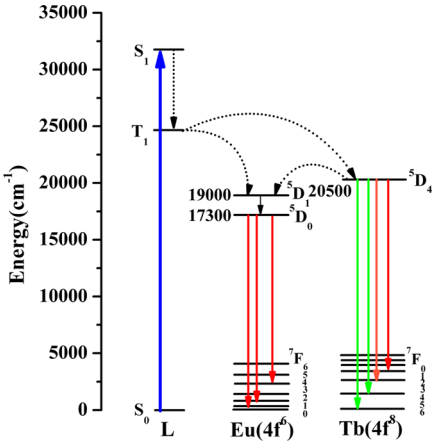

Figure 6. Energy level scheme showing energy transfer processes in compound **4**.

mechanism. The energy level scheme depicted in Figure 6 summarizes the intramolecular energy transfer processes taking place in heterodinuclear coordination compound **4**.

CONCLUSIONS

In this Article, we have reported the self-assembly synthesis, crystal structures, and photoluminescent properties of four new homodinuclear and heterodinuclear lanthanide (Ln = Eu, Tb, Gd, EuTb) coordination compounds derived from a novel amide ligand, benzyl-*N*,*N*-bis[(2′-furfury-laminoformyl)-phenoxyl)ethyl]-amine (**L**). The single-crystal X-ray diffraction analyses have revealed the isostructural character of all the lanthanide derivatives **1**−**4**, which are composed of zero-dimensional (0D) rectangular macrocycle blocks. Moreover, an interesting feature of EuTb heterodinuclear derivative **4** consists of the assembly of discrete dinuclear 0D units into a 2D H-bonded network with the **sql** topology, which has not yet been identified in a heterometallic EuTb compound. Under the excitation, both complexes **1** and **2** can show the characteristic luminescence emissions of the central Eu(III) and Tb(III) ions. The relative intensities and overall luminescence quantum yields show that the ligand **L** can effectively sensitize the luminescence of Tb(III) rather than Eu(III). Another noteworthy feature of the current study concerns a Tb(III)-to-Eu(III) energy transfer ability of the heterodinuclear compound **4**, which has been investigated in detail by the measurement of the energy levels of the ligand **L** and the luminescence lifetimes of the excited-state energy levels of the central Eu(III) and Tb(III) ions. We believe the obtained results should deserve further exploration, namely toward the construction of lanthanide based color displays, luminescence sensors, and photonic devices.

EXPERIMENTAL SECTION

Materials and Instrumentation. Lanthanide nitrates were prepared by dissolving Eu_2O_3 (99.99%, Shanghai Yuelong) in nitric acid (7 mol L^{-1}) followed by successive evaporating to remove excess acid. *N*-Furfurylsalicylamide[33] was synthesized on the basis of the literature. Other chemicals were all commercially available and purified by standard methods. Elemental analyses were conducted using an Elementar Vario EL. The amounts of lanthanide ions in complexes **1**−**4** were tested by inductively coupled plasmas (ICP) which were recorded on IRIS Advantage ER/S spectrophotometer. Thermogravimetric analyses (TGA) and differential scanning calorimetry (DSC) were performed using a STA 449C thermal analyzer up to 900 °C at a heating rate of 10 °C min^{-1} under air. Mass spectra were recorded on a Bruker UHR-TOF maXis 4G mass spectrometer. The FT-IR spectra were recorded on a Nicolet Nexus 670 instrument in the 4000−400 cm^{-1} region using KBr pellets. ^{1}H NMR (400 MHz) and ^{13}C NMR (100 MHz) spectra were obtained with a Bruker Avance 400 spectrometer in $CDCl_3$ solutions, with tetramethylsilane ($Si(CH_3)_4$) as an internal standard. Absorption spectra were measured on a Varian UV-Cary100 spectrophotometer. The steady-state luminescence spectra and the lifetime measurements were measured on an Edinburgh Instruments FSL920 fluorescence spectrometer, with 450 W Xe arc lamp as the steady-state excitation source or Nd-pumped OPOlette laser as the excitation source for lifetime measurements. The 77 K phosphorescence spectrum was recorded on a Hitachi F-4500 fluorescence spectrophotometer. The quantum yields of the complexes in the solid state were determined according to an absolute method of Wrighton[34] using an integrating sphere (150 mm diameter, $BaSO_4$ coating) from Edinburgh Instruments FLS920. Three parallel measurements were carried out for each sample, so that the presented value corresponds to the arithmetic mean value. The errors in the quantum yield values associated with this technique were estimated to be within 10%. The lifetime measurement was obtained on an Edinburgh Instruments FLS920 fluorescence spectrometer using a Nd pumped OPOlette laser as the excitation source. EDX analysis was carried out with a scanning electron microscope, Hitachi S-4800, Chiyoda-ku, Japan.

Synthesis of the Benzyl-*N*,*N*-bis[(2′-furfurylaminoformyl)-phenoxyl)ethyl]-amine (L). The *β*,*β*′-dichlorodiethylamine hydrochloride salt (0.174 g, 1 mmol) and potassium carbonate (0.276 g, 2 mmol) were refluxed in acetone (25 cm^3) for 30 min, and then the benzyl bromide (0.171 g, 1 mmol) was added to the solution. The hot solution was filtered off after refluxing for 12 h. The product was obtained after solvent was removed under reduced pressure. The above product was added to a mixture of *N*-furfurylsalicylamide (0.492 g, 2 mmol), potassium carbonate (0.552 g, 4 mmol), and distilled dimethylformamide (DMF) (20 cm^3) and then warmed to 90 °C stirring for 12 h. The mixture was poured into water (100 cm^3) after cooling to room temperature. The product was extracted into dichloromethane, washed with brine, dried over Na_2SO_4, and concentrated under reduced pressure. The residue was purified by silica gel chromatography to obtain **L** as a white solid. Yield: 76%, mp 81−83 °C. Anal. Calcd for $C_{35}H_{35}O_6N_3$: C, 70.81; H, 5.94; N, 7.08. Found: C, 70.72; H, 6.10; N, 6.89. IR (KBr pellet, cm^{-1}): 3330 m, 2930 w, 1640 s ν(C═O), 1600 w, 1529 s, 1489 w, 1450 w, 1307 w, 1240 m, 1157 w, 1107 w, 1041 w, 754 w, 732 w, 656 w, 518 w. ^{1}H NMR ($CDCl_3$, 400 MHz): δ 8.37 (s, 2H), 8.20 (dd, 2H, J = 8 Hz), 7.38 (t, 2H, J = 6.8 Hz), 7.27 (s, 7H), 7.06 (t, 2H, J = 7.4 Hz), 6.78 (d, 2H, J = 8.0 Hz), 6.27 (dd, 2H, J = 4.8 Hz), 6.22 (d, 2H, J = 2.8 Hz), 4.60 (d, 4H, J = 5.2 Hz), 4.10 (t, 4H, J = 6.0 Hz), 3.70 (s, 2H), 2.95 (t, 4H, J = 5.6 Hz). ^{13}C NMR ($CDCl_3$, 100 MHz): δ 165.1, 156.4, 151.8, 141.9, 137.9, 132.8, 132.4, 128.8, 128.5, 127.5, 121.6, 121.5, 112.4, 107.4, 66.6, 59.1, 53.4. 36.8. MS (ESI$^+$): m/z 594 (M + H)$^+$.

Synthesis of the Lanthanide Complexes 1−4. *[Ln$_2$(μ_2-L)$_2$(NO$_3$)$_6$(EtOH)$_2$] (1−3).* An ethyl acetate solution (5 cm^3) of $Ln(NO_3)_3{\cdot}6H_2O$ [Ln = Eu (0.045 g, 0.1 mmol for **1**), Tb (0.045 g, 1 mmol for **2**), and Gd (0.045 g, 0.1 mmol for **3**)] was dropped into a solution of **L** (0.059 g, 0.1 mmol in ethyl acetate (5 cm^3). The mixture was filtered off after stirred at r.t. for 4 h. After washing with ethyl acetate three times, complexes **1**−**3** were furnished by dried *in vacuo* under P_4O_{10} for two days, yield: 62−75%. Elemental analysis details follow. Found for **1**, $C_{74}H_{82}Eu_2N_{12}O_{32}$: C, 45.02; H, 3.83; N, 8.42; Eu, 15.25. Anal. Calcd: C, 45.45; H,4.23; N, 8.60, Eu, 15.55. Found for **2**, $C_{74}H_{82}Tb_2N_{12}O_{32}$: C, 44.83; H, 3.76; N, 8.44; Tb, 15.88. Anal. Calcd: C, 45.13; H, 4.20; N, 8.53; Tb, 16.14. Found for **3**, $C_{74}H_{82}Gd_2N_{12}O_{32}$: C, 44.89; H, 3.75; N, 8.24; Gd, 15.86. Anal. Calcd: C, 45.21; H, 4.20; N, 8.55; Gd, 16.00. The three complexes show essentially similar IR spectra, the characteristic bands of which have similar shifts, suggesting that they are structurally similar. IR details follow (KBr pellet, cm^{-1}). For complex **1**: 3356 m, 1671 s, 1615 s ν(C═O), 1595 m, 1566 m, 1494 s, 1474 s, 1383 w, 1307 s, 1236 w, 1111 w, 1029 m, 760 s. For complex **2**: 3356 m, 1671 s, 1620 s ν(C═O), 1595 m, 1566 m, 1494 s,

dx.doi.org/10.1021/ic402338q | *Inorg. Chem.* 2014, 53, 935−942

Table 3. Crystal Data and Structure Refinements for Compounds 1−4

	1	2	3	4
empirical formula	$C_{74}H_{82}Eu_2N_{12}O_{32}$	$C_{74}H_{82}Tb_2N_{12}O_{32}$	$C_{74}H_{82}Gd_2N_{12}O_{32}$	$C_{74}H_{82}EuN_{12}O_{32}Tb$
fw	1955.44	1969.36	1966.02	1962.40
cryst syst	monoclinic	monoclinic	monoclinic	monoclinic
space group	$P2_1/c$	$P2_1/c$	$P2_1/c$	$P2_1/c$
a (Å)	16.338(4)	16.338(4)	16.287(8)	16.345(9)
b (Å)	13.490(3)	13.490(3)	13.456(6)	13.493(7)
c (Å)	19.958(5)	19.958(5)	19.899(9)	19.954(11)
α (deg)	90.00	90.00	90.00	90.00
β (deg)	104.485(2)	104.485(2)	104.544(5)	104.685(4)
γ (deg)	90.00	90.00	90.00	90.00
V (Å^3)	4258.7(16)	4258.7(16)	4221(3)	4257(4)
Z	2	2	2	2
D_{calcd} (g cm^{-3})	1.525	1.536	1.547	1.531
μ(Mo Kα) (mm^{-1})	1.549	1.737	1.648	1.643
F(000)	1984	1992	1988	1988
GOF on F^2	0.985	1.056	1.078	1.013
final R indices, [$I > 2\sigma(I)$]	R1 = 0.0497	R1 = 0.0455	R1 = 0.0566	$R1$ = 0.0515
	wR2 = 0.1230	wR2 = 0.1147	wR2 = 0.1360	wR2 = 0.1243
R indices (all data)	R1 = 0.0762	$R1$ = 0.0706	R1 = 0.1075	R1 = 0.0833
	wR2 = 0.1453	wR2 = 0.1347	wR2 = 0.1766	wR2 = 0.1450

1475 s, 1384 m, 1308 s, 1236 m, 1111 w, 1030 m, 760 s. For complex **3**: 3359 m, 1669 w, 1615 s ν(C═O), 1596 m, 1566 m, 1493 s, 1476 s, 1384 w, 1308 s, 1240 w, 1111 w, 1029 m, 756 s.

[EuTb(μ_2-L)$_2$(NO$_3$)$_6$(EtOH)$_2$] (4). An ethyl acetate solution (5 cm^3) of $Eu(NO_3)_3{\cdot}6H_2O$ (0.022 g, 0.05 mmol) and $Tb(NO_3)_3{\cdot}6H_2O$ (0.023 g, 0.05 mmol) was dropped into a solution of **L** (0.059 g, 0.1 mmol) in ethyl acetate (5 cm^3). The mixture was filtered off after stirring at r.t. for 4 h. After washing with ethyl acetate three times, product **4** was obtained by dried *in vacuo* under P_4O_{10} for two days, yield: 64%. Anal. Found for $C_{74}H_{82}EuN_{12}O_{32}Tb$: C, 44.97; H, 3.76; N, 8.25, Eu, 7.24; Tb, 7.82. Anal. Calcd.: C, 45.29; H, 4.21; N, 8.46; Eu, 7.75; Tb, 8.10. IR (KBr pellet, cm^{-1}): 3356 m, 3300 m, 1670 s, 1618 s ν(C═O)), 1566 s, 1494 s, 1474 s, 1374 m, 1307 s, 1237 m, 1029 m, 757 s.

Unfortunately, the reliable mass spectrometry data for complex **4** could not be obtained because the complex is rather unstable in solutions.

Single-Crystal X-ray Crystallography. Single crystals of the complexes were obtained using an anhydrous diethyl ether diffused into a mixed EtOH/MeCN solution of **1**−**4** for about two weeks at room temperature. The X-ray single-crystal measurements were carried out on a Bruker SMART CCD detector diffractometer at 294 K, using graphite-monochromatic Mo Kα radiation (λ = 0.710 73 Å). Semiempirical absorption corrections were applied using the SADABS program. The structures were solved by direct methods and refined by full-matrix least-squares on F^2 using the SHELXS-97 and SHELXL-97 programs.[35] Details of crystallographic parameters, data collection, and refinement for these complexes are listed in Table 3. Hydrogen bonds in crystal packing of **1**−**4** are listed in Table S2 (Supporting Information). Representative bond distances [Å] and angles [deg] are given in Table S4 (Supporting Information). CCDC 954976 (**1**), 954977 (**2**), 960612 (**3**), and 954978 (**4**) include all supplementary crystallographic data of these four new lanthanide complexes.

■ ASSOCIATED CONTENT

Supporting Information

CIF files with crystallographic data, selected bonding parameters and intramolecular $\pi-\pi$ and C−H···π stacking interactions, photophysical data, EDX analysis results and EDX spectrum, thermal analysis plots, FTIR spectra, absorption spectrum and phosphorescence spectrum, and low temperature and room temperature luminescence decay profiles. This material is available free of charge via the Internet at http://pubs.acs.org.

■ AUTHOR INFORMATION

Corresponding Author

*E-mail: tangyu@lzu.edu.cn. Phone: +86-931-8912552. Fax: +86-931-8912582.

Notes

The authors declare no competing financial interest.

■ ACKNOWLEDGMENTS

Financial support from the National Natural Science Foundation of China (Projects 21071068, 20931003) and the National Science Foundation for Fostering Talents in Basic Research of the National Natural Science Foundation of China (Project J1103307) is acknowledged. A.M.K. acknowledges the Foundation for Science and Technology (FCT), Portugal (PTDC/QUI-QUI/121526/2010, PEst-OE/QUI/UI0100/2013).

■ REFERENCES

(1) (a) Bünzli, J.-C. G. Rare Earth Luminescent Centers in Organic and Biochemical Compounds. In *Spectroscopic Properties of Rare Earths in Optical Materials*; Liu, G. K., Jacquier, B., Eds.; Springer-Verlag: Berlin, 2005; Vol. *83*, Chapter 11. (b) Cotton, S. *Lanthanide and Actinide Chemistry*; John Wiley & Sons: New York, 2006. (c) Jones, C. *D-And F-Block Chemistry*; Royal Society of Chemistry: London, 2000. (d) Bünzli, J.-C. G. *Acc. Chem. Res.* **2006**, *39*, 53. (e) Bünzli, J.-C. G.; Piguet, C. *Chem. Soc. Rev.* **2005**, *34*, 1048. (f) Santos, C. M. G.; Harte, A. J.; Quinn, S. J.; Gunnlaugsson, T. *Coord. Chem. Rev.* **2008**, *252*, 2512. (g) Zheng, X. L.; Liu, Y.; Pan, M.; Lu, X. Q.; Zhang, J. Y.; Zhao, C. Y.; Tong, Y. X.; Su, C. Y. *Angew. Chem., Int. Ed.* **2007**, *46*, 7399. (h) Mizukami, S.; Tonai, K.; Kaneko, M.; Kikuchi, K. *J. Am. Chem. Soc.* **2008**, *130*, 14376. (i) Keizers, P. H. J.; Saragliadis, A.; Hiruma, Y.; Overhand, M.; Ubbink, M. *J. Am. Chem. Soc.* **2008**, *130*, 14802. (j) Guo, Y. L.; Dou, W.; Zhou, X. Y.; Liu, W. S.; Qin, W. W.; Zang, Z. P.; Zhang, H. R.; Wang, D. Q. *Inorg. Chem.* **2009**, *48*, 3581. (k) Petoud, S.; Cohen, S. M.; Bünzli, J.-C. G.; Raymond, K. N. *J. Am. Chem. Soc.* **2003**, *125*, 13324. (l) Song, X. Q.; Zhou, X. Y.; Liu, W. S.; Dou, W.; Ma, J. X.; Tang, X. L.; Zheng, J. R. *Inorg. Chem.* **2008**, *47*, 11501. (m) Wang, Q.; Tang, K. Z.; Liu, W. S.; Tang, Y.; Tan, M. Y. *Eur. J. Inorg. Chem.* **2010**, 5318. (n) Xu, J.; Jia, L.; Jin, N. Z.; Ma, Y. F.; Liu, X.; Wu, W. Y.; Liu, W. S.; Tang, Y.; Zhou, F. *Chem.—Eur. J.* **2013**, *19*, 4556.

(2) (a) Moore, E. G.; Xu, J.; Jocher, C. J.; Werner, E. J.; Raymond, K. N. *J. Am. Chem. Soc.* **2006**, *128*, 10648. (b) Moore, E. G.; Xu, J.; Jocher, C. J.; Castro-Rodriguez, I.; Raymond, K. N. *Inorg. Chem.* **2008**, *47*, 3105.
(3) (a) Liu, C.; Wang, M.; Zhang, T.; Sun, H. *Coord. Chem. Rev.* **2004**, *248*, 147. (b) Weibel, N.; Charbonnère, L.; Guardigli, M.; Roda, A.; Ziessel, R. *J. Am. Chem. Soc.* **2004**, *126*, 4888.
(4) Thomson, M. K.; Doble, D. M. J.; Tso, L. S.; Barra, S.; Botta, M.; Aime, S.; Raymond, K. N. *Inorg. Chem.* **2004**, *43*, 8577.
(5) Piggot, P. M. T.; Hall, L. A.; White, A. J. P.; Williams, D. J. *Inorg. Chem.* **2003**, *42*, 8344.
(6) (a) Lis, S.; Elbanowski, M.; Ma-kowska, B.; Hnatejko, Z. *J. Photochem. Photobiol., A* **2002**, *150*, 233. (b) Piguet, C.; Bünzli, J.-C. G. *Chem. Soc. Rev.* **1999**, *28*, 347. (c) Faulkner, S.; Pope, S. J. A. *J. Am. Chem. Soc.* **2003**, *125*, 10526. (d) Brittain, H. G. *Inorg. Chem.* **1978**, *17*, 2762. (e) Chrysochoos, J. *J. Lumin.* **1974**, *9*, 79.
(7) (a) Santos, A. M.; Marques, F. M. B.; Carlos, L. D.; Rocha, J. *J. Mater. Chem.* **2006**, *16*, 3139. (b) Zhang, T.; Xu, Z.; Qian, L.; Teng, F.; Xu, X. R. *J. Appl. Phys.* **2005**, *98*, 3503. (c) Irfanullah, M.; Iftikhar, K. *Inorg. Chem. Commun.* **2010**, *13*, 694.
(8) (a) Ishizaka, T.; Nozaki, R.; Kurokawa, Y. *J. Phys. Chem. Solids* **2002**, *63*, 613. (b) Li, Q.; Li, T.; Wu, J. G. *J. Phys. Chem. B* **2001**, *105*, 12293.
(9) (a) Tremblay, M. S.; Halim, M.; Sames, D. *J. Am. Chem. Soc.* **2007**, *129*, 7570. (b) Luo, Y.; Calvez, G.; Freslon, S.; Bernot, K.; Daiguebonne, C.; Guillou, O. *Eur. J. Inorg. Chem.* **2011**, *50*, 3705. (c) Rao, X. T.; Huang, Q.; Yang, X. L.; Cui, Y. J.; Yang, Y.; Wu, C. D.; Chen, B. L.; Qian, G. D. *J. Mater. Chem.* **2012**, *22*, 3210. (d) Ida, S.; Ogata, C.; Eguchi, M.; Youngblood, W. J.; Mallouk, T. E.; Matsumoto, Y. *J. Am. Chem. Soc.* **2008**, *130*, 7052.
(10) Ramya, A. R.; Sharma, D.; Natarajan, S.; Reddy, M. L. P. *Inorg. Chem.* **2012**, *51*, 8818.
(11) Blatov, V. A. *IUCr CompComm Newsletter* **2006**, *7*, 4.
(12) (a) Blatov, V. A.; Proserpio, D. M. In *Modern Methods of Crystal Structure Prediction*; Oganov, A. R., Ed.; Wiley: New York, 2010; pp 1−28. (b) Blatov, V. A.; O'Keeffe, M.; Proserpio, D. M. *CrystEngComm* **2010**, *12*, 44. (c) Alexandrov, E. V.; Blatov, V. A.; Kochetkova, A. V.; Proserpio, D. M. *CrystEngComm* **2011**, *13*, 3947. (d) O'Keeffe, M.; Yaghi, O. M. *Chem. Rev.* **2012**, *112*, 675.
(13) The Reticular Chemistry Structure Resource (RCSR) Database: O'Keeffe, M.; Peskov, M. A.; Ramsden, S. J.; Yaghi, O. M. *Acc. Chem. Res.* **2008**, *30*, 1782.
(14) For recent examples of Eu and/or Tb compounds with the **sql** topology, see: (a) Amghouz, Z.; Garcia-Granda, S.; Garcia, J. R.; Ferreira, R. A. S.; Mafra, L.; Carlos, L. D.; Rocha, J. *Inorg. Chem.* **2012**, *51*, 1703. (b) Yang, A. H.; Gao, H. L.; Cui, J. Z.; Zhao, B. *CrystEngComm* **2011**, *13*, 1870. (c) Chen, S.; Fan, R. Q.; Sun, C. F.; Wang, P.; Yang, Y. L.; Su, Q.; Mu, Y. *Cryst. Growth Des.* **2012**, *12*, 1337. (d) Ding, F.; Song, X.; Jiang, B.; Smet, P. F.; Poelman, D.; Xiong, G.; Wu, Y. L.; Gao, E. J.; Verpoort, F.; Sun, Y. G. *CrystEngComm* **2012**, *14*, 1753. (e) Henry, N.; Costenoble, S.; Lagrenee, M.; Loiseau, T.; Abraham, F. *CrystEngComm* **2011**, *13*, 251. (f) Ladner, L.; Ngo, T.; Crawford, C.; Assefa, Z.; Sykora, R. E. *Inorg.Chem.* **2011**, *50*, 2199.
(15) See the Cambridge Structural Database (CSD, version 5.34, May 2013): Allen, F. H. *Acta Crystallogr.* **2002**, *B58*, 380.
(16) (a) Shyni, R.; Biju, S.; Reddy, M. L. P.; Cowley, A. H.; Findlater, M. *Inorg. Chem.* **2007**, *46*, 11025. (b) Biju, S.; Raj, D. B. A.; Reddy, M. L. P.; Kariuki, B. M. *Inorg. Chem.* **2006**, *45*, 10651.
(17) (a) Ambili Raj, D. B.; Francis, B.; Reddy, M. L. P.; Butorac, R. R.; Lynch, V. M.; Cowley, A. H. *Inorg. Chem.* **2010**, *49*, 9055. (b) Divya, V.; Biju, S.; Luxmi Varma, R.; Reddy, M. L. P. *Dalton Trans.* **2010**, *20*, 5220. (c) Francis, B.; Ambili Raj, D. B.; Reddy, M. L. P. *Dalton Trans.* **2010**, *39*, 8084.
(18) (a) Sun, Y. Q.; Zhang, J.; Yang, G. Y. *Chem. Commun.* **2006**, 4700. (b) Kirby, A. F.; Foster, D.; Richardson, F. S. *Chem. Phys. Lett.* **1983**, *95*, 507.
(19) (a) Remya, P. N.; Biju, S.; Reddy, M. L. P.; Cowley, A. H.; Findlater, M. *Inorg. Chem.* **2008**, *47*, 7396. (b) Xia, J.; Zhao, B.; Wang, H. S.; Shi, W.; Ma, Y.; Song, H. B.; Cheng, P.; Liao, D. Z.; Yan, S. P. *Inorg. Chem.* **2007**, *46*, 3450. (c) Dieke, G. H. *Spectra and Energy levels of Rare Earth Ions in Crystals*; Interscience: New York, 1968. (d) Lucky, M. V.; Sivakumar, S.; Reddy, M. L. P.; Paul, A. K.; Natarajan, S. *Cryst. Growth Des.* **2011**, *11*, 857.
(20) (a) Aiga, F.; Iwanaga, H.; Amano, A. *J. Phys. Chem. A* **2005**, *109*, 11312. (b) He, P.; Wang, H. H.; Liu, S. G.; Shi, J. X.; Wang, G.; Gong, M. L. *Inorg. Chem.* **2009**, *48*, 11382. (c) Regulacio, M. D.; Pablico, M. H.; Vasquez, J. A.; Myers, P. N.; Gentry, S.; Prushan, M.; Tam-Chang, S. W.; Stoll, S. L. *Inorg. Chem.* **2008**, *47*, 1512. (d) Bazzicalupi, C.; Bencini, A.; Bianchi, A.; Giorgi, C.; Fusi, V.; Masotti, A.; Valtancoli, B.; Roque, A.; Pina, F. *Chem. Commun.* **2000**, 561. (e) Sabbatini, N.; Guardigli, M.; Lehn, J. M. *Coord. Chem. Rev.* **1993**, *123*, 201.
(21) Steemers, F. J.; Verboom, W.; Reinhoudt, D. N.; Vander Tol, E. B.; Verhoeven, J. W. *J. Am. Chem. Soc.* **1995**, *117*, 9408.
(22) (a) Latva, M.; Takalo, H.; Mukkala, V.-M.; Matachescu, C.; Rodríuez-Ubis, J. C.; Kankare, J. *J. Lumin.* **1997**, *75*, 149. (b) Arnaud, N.; Georges, J. *Spectrochim. Acta* **2003**, *59*, 1829.
(23) Gutierrez, F.; Tedeschi, C.; Maron, L.; Daudey, J. P.; Poteau, R.; Azema, J.; Tisnès, P.; Picard, C. *Dalton Trans.* **2004**, 1334.
(24) Ma, Y. F.; Wang, H. P.; Liu, W. S.; Wang, Q.; Xu, J.; Tang, Y. *J. Phys. Chem. B* **2009**, *113*, 14139.
(25) (a) Sivakumar, S.; Reddy, M. L. P.; Cowley, A. H.; Butorac, R. R. *Inorg. Chem.* **2011**, *50*, 4882. (b) Sivakumar, S.; Reddy, M. L. P.; Cowley, A. H.; Vasudevan, K. V. *Dalton Trans.* **2010**, *39*, 776. (c) Raphael, S.; Reddy, M. L. P.; Cowley, A. H.; Findlater, M. *Eur. J. Inorg. Chem.* **2008**, *28*, 4387.
(26) Ramya, A. R.; Reddy, M. L. P.; Cowley, A. H.; Vasudevan, K. V. *Inorg. Chem.* **2010**, *49*, 2407.
(27) (a) Xiao, M.; Selvin, P. R. *J. Am. Chem. Soc.* **2001**, *123*, 7067. (b) Quici, S.; Cavazzini, M.; Marzanni, G.; Accorsi, G.; Armaroli, N.; Ventura, B.; Barigelletti, F. *Inorg. Chem.* **2005**, *44*, 529.
(28) (a) Shavaleev, N. M.; Eliseeva, S. V.; Scopelliti, R.; Bünzli, J.-C. G. *Inorg. Chem.* **2010**, *49*, 3927. (b) Zucchi, G.; Olivier, M.; Pierre, T.; Gumy, F.; Bünzli, J.-C. G.; Michel, E. *Chem.—Eur. J.* **2009**, *15*, 9686.
(29) Pavithran, R.; Saleesh Kumar, N. S.; Biju, S.; Reddy, M. L. P.; Alves, S., Jr.; Freire, R. O. *Inorg. Chem.* **2006**, *45*, 2184.
(30) Nasso, I.; Bedel, S.; Galaup, C.; Picard, C. *Eur. J. Inorg. Chem.* **2008**, *12*, 2064.
(31) Choppin, G. R.; Bünzli, J.-C. G. *Lanthanide Probes in Life, Chemical and Earth Sciences*; Elsevier Publishing Co.: Amsterdam, 1989; Chapter 7.
(32) Piguet, C.; Büunzli, J.-C. G.; Bernardinelli, G.; Hopfgartner, G.; Williams, A. F. *J. Am. Chem. Soc.* **1993**, *115*, 8197.
(33) Michio, K. *Bull. Chem. Soc. Jpn.* **1976**, *49*, 2679.
(34) (a) Wrighton, M. S.; Ginley, D. S.; Morse, D. L. *J. Phys. Chem.* **1974**, *78*, 2229−2233. (b) de Mello, J. C.; Wittmann, H. F.; Friend, R. H. *Adv. Mater.* **1997**, *9*, 230−232. (c) Greenham, N. C.; Samule, I. D. W.; Hayes, G. R.; Philips, R. T.; Kessener, Y. A. R. R.; Moratti, S. C.; Holmes, A. B.; Friend, R. H. *Chem. Phys. Lett.* **1995**, *241*, 89−96.
(35) (a) Sheldrick, G. M. *Acta; Crystallogr., Sect. A* **1990**, *46*, 467. (b) Sheldrick, G. M. *SHELXS-97, A Program for X-ray Crystal Structure Solution, and SHELXL-97, A Program for X-ray Structure Refinement*; Göttingen University: Göttingen, Germany, 1997.